

# Oil shale pyrolysis and electric heating in situ mining technology improvements

Yi Pan<sup>(a)</sup>, Xukun Fan<sup>(a)</sup>, Shuangchun Yang<sup>(a)</sup>, Zhiyong Hu<sup>(a)\*</sup>, Yulin Yan<sup>(b)</sup>

<sup>(a)</sup> College of Petroleum and Natural Gas Engineering, Liaoning Petrochemical University, Fushun, Liaoning 113001, China

<sup>(b)</sup> Fushun Mining Group Co., Ltd., 25 Central Street, Xinfu District, Fushun, Liaoning 113000, China

Received 30 April 2024, accepted 18 October 2024, available online 31 October 2024

**Abstract.** *In the engineering of oil shale, in situ extraction technology using electric heating involves heating the oil shale reservoir with an electric heater at high temperatures to convert the solid kerogen in oil shale into liquid hydrocarbons. These liquid hydrocarbons are then extracted from underground using traditional oil and gas drilling and production techniques. This paper discusses the pyrolysis mechanism, pore evolution, mineral transformation, and classification of electric heating technology for oil shale. It also summarizes research progress aimed at improving in situ extraction technology for oil shale, providing valuable insights for further research and development in this field.*

**Keywords:** *oil shale pyrolysis, electric heating, well pattern, electric heater, kerogen.*

## 1. Introduction

Energy and the environment form the foundation of human social activities, with ample energy and a healthy environment serving as essential guarantees for a country's prosperity and long-term stability. As traditional fossil fuel reserves, such as coal, oil, and natural gas, continue to diminish, it is increasingly important to focus on unconventional energy sources due to the inability of new energy sources to immediately compensate for the shortfall [1]. After the COVID-19 pandemic, global economic recovery and sustained growth have driven global oil demand to reach a new peak. In 2023, global oil demand surged by 2.1 million barrels per day compared to the previous year, reaching 101.7 million barrels per day and surpassing the pre-pandemic

\* Corresponding author, [huzhiyong024@163.com](mailto:huzhiyong024@163.com)

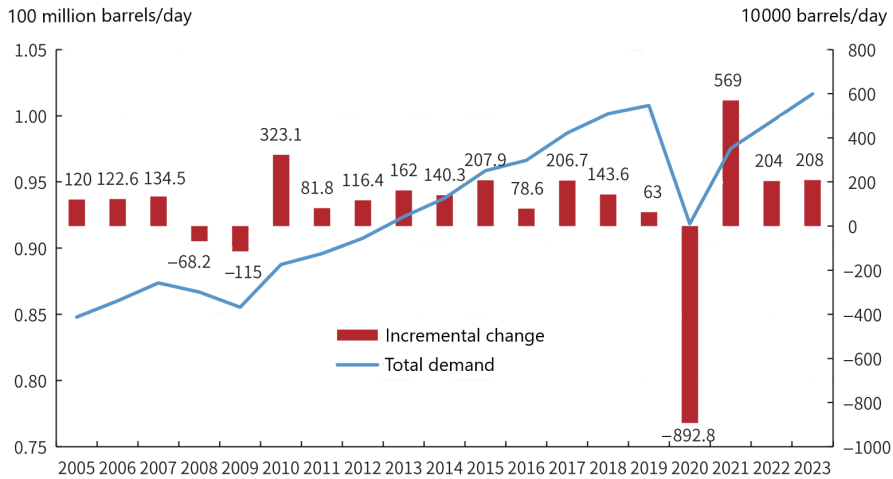


Fig. 1. Global oil demand and incremental changes in 2005–2023 [2].

level of 100.8 million barrels per day in 2019 [2], as shown in Figure 1. Unconventional oil reserves have thus emerged as a significant global energy source, prompting countries to progressively intensify their exploration of these resources.

Unlike conventional oil and gas reservoirs, unconventional oil and gas reservoirs are mainly distributed continuously in slopes or protrusions of sedimentary basins [3]. Oil shale, formed by the deposition of organic matter over millions of years, is an extremely important part of unconventional oil and gas resources. Rich in organic matter and inorganic minerals, oil shale's main component is kerogen, which is distilled and heated to produce shale oil [4, 5].

Initially, dry retorting technology for oil shale focused on crushing the shale into small pieces and heating it in a specific space to obtain shale oil. However, field tests revealed poor economic benefits, prompting the need for in situ dry retorting technology [6]. This approach involves heating the oil shale in its formation using electric heaters, high-temperature fluids, and injected air to ignite the shale, causing it to crack and produce shale oil and pyrolysis gas [7–9]. These products are then transported to the surface through production wells.

Various technical prospects have been explored in the development, research, and industrial application of in situ dry retorting technology, leading to the development of many feasible technologies. However, due to cost issues, most of these technologies have only advanced as far as laboratory research and pilot testing. One exception is the ICP (in situ conversion process) technology, which has been proven feasible for oil shale in situ mining through electric heating through more than 20 years of on-site testing [10]. Furthermore, this

method offers advantages that other in situ mining technologies cannot match: its relative maturity ensures easy control over the heating process, despite slower speed and considerable heat loss.

Compared to traditional surface retorting methods, electric heating-based in situ extraction is less harmful to the environment and consumes less water. Additionally, it can increase the value added of mineral resources by opening new growth points and prolonging the service life of mining areas. The quality of oil produced from oil shale using electric heating technology is suitable for large-scale industrial applications and enables extraction from deeper layers.

This paper presents an in-depth exploration of in situ oil shale extraction technology utilizing electric heating, as well as an analysis of the oil shale pyrolysis mechanism and associated technical advancements. Through a comprehensive examination of the pyrolysis mechanism, pore evolution, and mineral transformation within oil shale, this study identifies key factors influencing the pyrolysis efficiency of electrically heated oil shale. Furthermore, it outlines the technical enhancements implemented based on these critical factors.

## **2. Pyrolysis mechanism, pore evolution, and product evolution of oil shale**

In the process of in situ oil shale thermal decomposition using oil shale electric heating technology, as the temperature of the electric heater increases, the outer layer adjacent to the heater initiates pyrolysis, leading to concurrent pyrolysis within the interior of the oil shale. This results in the generation of shale oil, pyrolysis gas, and residual carbon through fissures and pores. Therefore, when discussing the pyrolysis mechanism of oil shale, it is imperative to consider not only its chemical evolution but also the structural changes in pores and fissures during this process.

### **2.1. Pyrolytic properties of oil shale**

The pyrolysis of oil shale occurs at elevated temperatures, initiating a series of intricate physical and chemical reactions. Throughout this process, various phenomena, such as the cleavage of cross-linked bonds and reorganization of products, are observed [11]. Thermal cracking leads to the transformation of organic matter in oil shale into shale oil, thermal cracking gas, semi-coke solid residue, and residual carbon. The mechanism of thermal cracking involves the medium-temperature cracking reaction of organic matter in oil shale, comprising two primary components: the thermal cracking of oil shale organic matter (kerogen) into asphalt and subsequent conversion of asphalt into shale oil, shale gas, and residual carbon [12, 13].

## 2.2. Pore evolution during oil shale pyrolysis

The porosity and permeability of oil shale are usually very poor. However, pyrolysis can greatly improve the storage capacity of oil, though this increase in porosity does not occur immediately during the process [14]. The vaporized shale oil, converted from kerogen, is not released continuously or steadily. When the pyrolysis time is short or the heating temperature is low, only a small part of the organic matter can be released, and the residual solidified colloidal substances after decomposition and shale oil components within the semi-coke particles may block the pores and cracks [15]. As pyrolysis time and temperature increase, the organic matter blocked in the particle pores is pyrolyzed into low molecular weight compounds, and finally vaporizes from the particles and opens the blocked orifice. Pores become larger [16].

Saif et al. used micro-CT to study the pyrolysis process of the Green River oil shale and confirmed this observation [17, 18]. Even after observing different pyrolysis temperatures, they found that the number of pores increased sharply when the critical temperature reached 390–400 °C, which was basically consistent with the onset of kerogen cracking. Tiwari et al. used micro-CT and lattice Boltzmann simulation to observe the pores of oil shale before and after pyrolysis [19], and found that the porosity of oil shale depends on the distribution of kerogen [20]. In light oil shale, rich in kerogen, porosity can reach up to 38%, while in dark oil shale, rich in minerals, porosity is only 12%.

As the heating temperature continues to increase, reaching 520 °C, kerogen gradually matures during the heating process, leading to the production of low molecular weight hydrocarbons. In the test conducted by He et al. on Fuyu and Nong'an oil shale samples, the methane content reached an astonishing 98.09 and 98.69%, respectively [21], and the porosity continued to increase. Bai et al. found that when the temperature reached 800 °C, the porosity of Huadian oil shale semi-coke soared to an impressive 60% [22], which is much higher than the porosity observed at 500 °C in Huadian oil shale, as tested by Kang et al. [23]. The reason is that the fixed carbon in oil shale is completely pyrolyzed at 800 °C, which leads to significant pore development in the semi-coke. These studies describe the characteristics of oil shale pyrolysis and kerogen cracking, proving the feasibility of in situ oil shale mining through electric heating.

## 2.3. Product evolution in oil shale pyrolysis

During pyrolysis, the decomposition of kerogen and hot asphalt does not occur simultaneously; rather, it takes place at distinct temperature intervals under different pyrolysis conditions. The speed and rate of product formation in oil shale at various temperatures can be categorized into three stages [21]:

- 1) Low-temperature mass loss stage: typically occurs from room temperature to 200–300 °C, accounting for approximately 3% of total mass

loss. This stage is primarily attributed to water evaporation, with a minor contribution from the decomposition of salts, such as sodium bicarbonate.

2) Medium-temperature mass loss stage: generally observed between 200–300 °C and around 600 °C, representing about 20% of total mass loss and serving as the principal phase in oil shale decomposition. During this stage, the kerogen within the organic matter undergoes extensive thermal cracking, leading to a series of intricate physical and chemical transformations that yield oil and thermal cracking gas. Notably, the oil yield exhibits a significant increase as the temperature rises from 430 to 460 °C. Furthermore, there is a marginal rise in the overall oil yield within the temperature range of 460 to 520 °C, as depicted in Figure 2.

3) High-temperature mass loss stage: typically occurs above 600 °C, constituting roughly 3% of total mass loss. The predominant processes during this phase involve the fracturing of carbonate minerals, such as calcite, dolomite, and iron-rich dolomite. Concurrently, the fixed carbon present in the oil shale undergoes high-temperature carbonization, producing  $\text{CO}_2$ , which reacts with fixed carbon to generate limited amounts of volatile gases, such as CO.

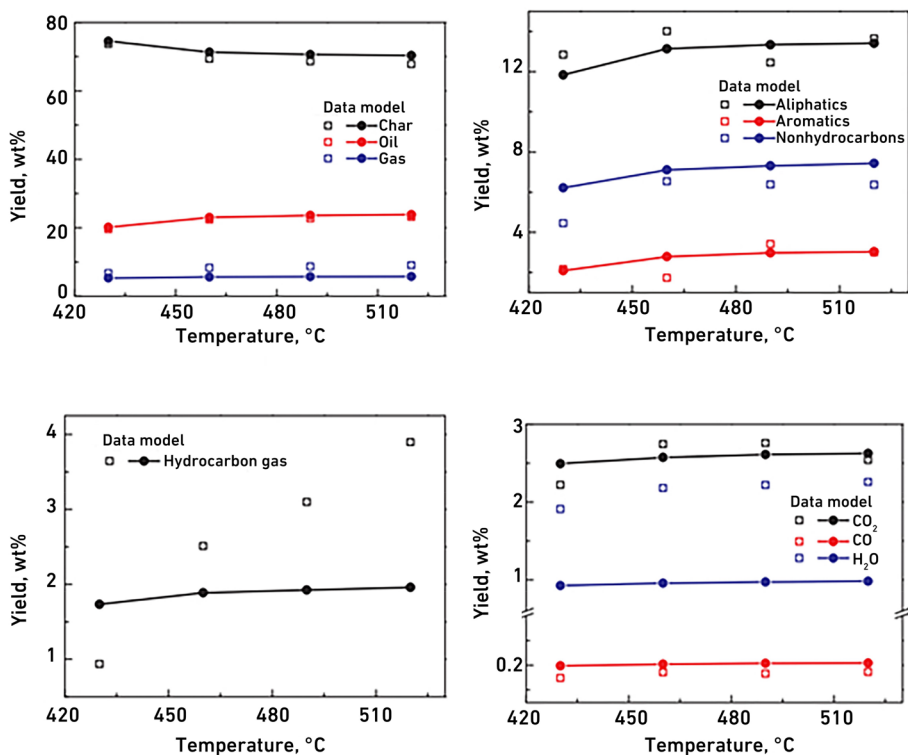


**Fig. 2.** Product distribution of Huadian oil shale at different temperatures in a fixed bed [24]. The color figure is available in the online version of this journal.

### **3. In situ oil shale mining technology using electric heating and its improvements**

Electric heating is a process that transforms electrical energy into thermal energy by stimulating molecules. The existing in situ extraction technologies for oil shale using electric heating encompass the ICP, Electrofrac™, geothermal fuel cell (GFC), and high-voltage power frequency electric heating (HVF). To enhance the efficiency of oil shale pyrolysis and maximize economic benefits, recent research has focused on optimizing well pattern distribution, refining the material structure of electric heating devices, and enhancing cementing materials.

#### **3.1. Research methods for in situ oil shale transformation technology using electric heating**

In situ oil shale electric heating technology has been developed as a potential alternative to the economically unfeasible oil shale surface retorting technology. This method involves drilling into the deposit and utilizing electric heaters to provide additional heat within the formation, enabling the on-site refinement of oil shale to yield oil and natural gas. However, it should be noted that this approach necessitates a longer processing time, with oil production achievable after two years of heating and mining becoming feasible after five years. Consequently, significant cost implications have arisen for research endeavors in this area. As a result, many researchers are currently focusing on small-scale experiments and simulations to investigate and refine electric heating methods for oil shale.

#### **3.2. Classification of in situ mining techniques for oil shale using electric heating**

The ICP technology utilizes subsurface in situ electric heating techniques. Multiple wells are drilled into the ground, categorized as heating wells, production wells, and monitoring wells. The electric heater within the heating well is employed to transfer heat to the oil shale, yielding oil and gas. Throughout the heating process, the fractured oil shale creates new pores and fractures, allowing for the flow of shale oil and pyrolysis gas through these channels to achieve enhanced thermal efficiency [25–28].

The Electrofrac™ technology is a specialized hydraulic fracturing technique designed for oil shale formations, involving the subsequent injection of conductive materials to create a resistive heating element. Upon application of electricity, the oil shale undergoes thermal cracking, yielding oil and gas, which are then recovered via production wells [28, 29].

The GFC technology utilizes the heat generated by solid oxide fuel cells to heat oil shale. Unlike other methods, this technology does not require large amounts of external energy, as it can provide its own energy [6, 28].

The HVF technology involves placing electrodes in the oil shale formation and applying high-voltage electricity to generate plasma and carbonized conductive channels within the oil shale. Subsequently, these conductive channels are heated by connecting the formation to a high-frequency electrical source, leading to the pyrolysis of the oil shale [28, 30, 31].

### 3.3. Improvement of in situ oil shale exploitation technology

The ICP technology, being the most widely utilized electric heating method, exhibits the highest feasibility. Consequently, efforts to enhance electric heating technology primarily center on refining the ICP technology. Wang et al. conducted simulations and comparisons of the Mitsui-hole and four-hole well types as well as a six-hole well type to ascertain variations in heating efficiency, ultimately determining that the six-hole well type demonstrated the swiftest temperature rise rate [32]. As shown in Figure 3, Fan et al. also found through simulation that the hexagonal well pattern achieves higher heating efficiency, with maximum efficiency obtained at a 2.5-meter heater spacing and a temperature of 340 °C [33]. Xia et al. supported this finding and proposed that heaters with smaller well spacing and higher power offer greater efficiency [34]. However, Li presented different views, finding that the optimal well spacing changes with heating time, and has a certain stage, which always increases with extended heating time [35]. These findings indicated that well structure exerts a significant influence on the heat conduction within electric heaters, thereby impacting the efficiency of the ICP technology for oil shale mining. This offers valuable insights for determining the optimal well type and spacing in future ICP technology production.

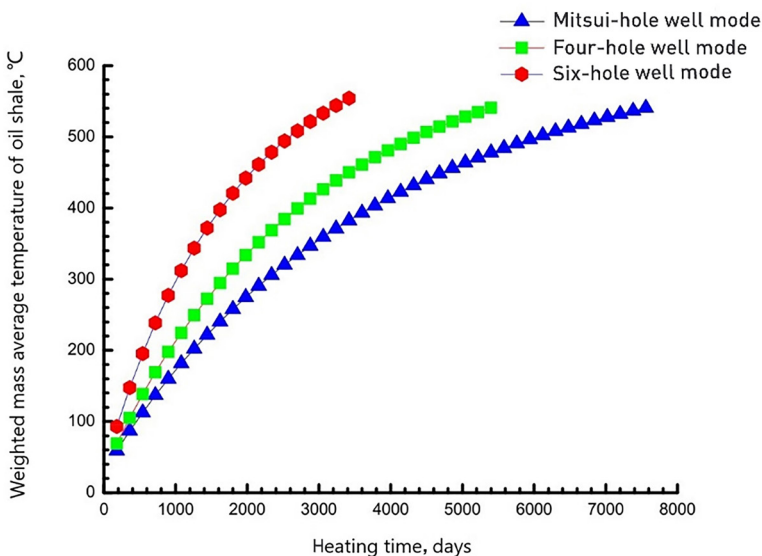


**Fig. 3.** Relationship between weighted average temperature and heating time of oil shale under different well patterns [33].

Some researchers have also used the method of adding catalysts to improve the ICP technology. Pei et al. proposed to increase convective heat transfer by adding easily available and inactive nitrogen ( $N_2$ ) into the reservoir [36], which had little effect on the downhole equipment and was easy to separate. After simulation, it was found that when the injection rate reached 400 m<sup>3</sup>/d, it could obtain 1.17 times the conventional ICP oil production. Additionally, adding porous aluminum silicate to promote the secondary decomposition of asphalt produced by oil shale has been shown to improve the conversion rate of hydrocarbon generation [37]. Sun et al. found that the exchange of heating and production wells can save the time required for heating and energy consumption, and is conducive to the improvement of the oil production rate [38]. Their research supports optimizing convective heating after the thermal cracking of oil shale, introducing catalysts for the promotion of thermal cracking, and transitioning heating and production wells to minimize heating duration.

Structural optimization of electric heaters is also an area of focus. Yue et al. found that shale oil yield increases with higher heating rates by studying the correlation between shale oil yield, temperature, and pyrolysis residence time of Yaojie oil shale [39]. Wang et al. studied the heating rates of Huadian oil shale in the range of 10–100 K/min across temperatures from 25 to 900 °C, finding consistent weight loss rates at basically all temperatures. With further research on the pyrolysis temperature of oil shale [40], new progress has been made in temperature optimization for the ICP electric heating technology [41]. New thermal conductive materials [42] and new wire mesh reactors [43] have been successfully used for in situ oil shale mining using electric heating [44].

Sandberg et al. used an improved ceramic material technology to make the heater work at a higher voltage, and also matched the casing technology used to increase the total length of the heater, which improved the work efficiency in the well site [44]. Zeng et al. selected copper, stainless steel, and nickel-chromium alloy to make an axisymmetric U-tube and vacuum heating tube heater, so that it could inject and extract fluid while heating [36]. Evidently, the optimization of electric heating technology cannot be limited to electric heaters. From the perspective of cementing, Hao et al. developed a heat-resistant cementing material with a temperature tolerance of 600 °C, a compressive strength of more than 60 MPa, and an elastic modulus as low as 12 GPa [45]. Gao also expressed the corresponding view that composite materials should be used for cementing, and pre-stressed cementing should be added with thermal insulation measures to reduce the thermal stress of casing [46].

The flow form of the shell side of the electric heater is similar to that of a shell-and-tube heat exchanger. Therefore, the technology applied in the shell-and-tube heat exchanger can be used in the continuous helical baffle downhole electric heater. Different from the segmental baffles used in traditional heat exchangers, Liu et al. employed a helical baffle heat exchanger with a higher

heat transfer coefficient. Without considering the cost, the double-layer helical baffle heat exchanger has better comprehensive performance [47]. Wang et al. confirmed these findings through verification [48].

Building on this, Jian et al. investigated the spiral angles of discontinuous helical baffles, comparing the heat transfer performance of 20, 30, 40, and 50° spiral angles, and concluded that the heat exchanger with a spiral angle of 40° has the best performance [49]. However, Xiao pointed out that the 40° conclusion is only applicable to cases where water is the shell-side fluid; for fluids with a larger Prandtl number, a smaller angle scheme would be a better choice [50]. Furthermore, Yang et al. found that keeping the 40° angle unchanged while increasing the number of sealing strips can improve heat transfer performance [51]. Wang et al. proposed the use of baffles to block the triangular leakage zone between two adjacent flat baffles [52]. Dong et al. and Chen et al. suggested using a three-point circumferential overlapping baffle scheme with a 20° inclination angle [53, 54]. This is because the shape of the three-point baffle is highly suitable for the equilateral triangular arrangement of tubes, and there is a row of tubes in each circumferential overlapping area of adjacent baffles to suppress the leakage flow [55–57]. By adopting a single-side shell-and-tube heat exchanger with double-layer continuous helical baffles without inner and outer sleeves, Yang et al. placed the inner and outer continuous helical baffles on different helical surfaces to ensure the formation of complex flow fields in the shell side [58].

Maakoul et al. improved the helical baffle design by developing a three-leaf-hole baffle with better heat transfer performance and greater pressure [59]. Dong et al. further modified the three-point circumferential overlapping baffle, using the least rods to support the inclined baffle, which simplified the manufacturing process of the jumper and effectively inhibited the reverse leakage in the triangular area between adjacent baffles [60]. Yang et al. connected the continuous helical baffles in series with the conventional segmental baffles. This configuration featured an arched inner shell side and continuous helical outer shell side, resulting in a better heat transfer coefficient [61]. Chen et al. further investigated the efficiency of three-point circumferential overlapping baffles, finding that when the baffles were designed with 16 root canals and a 12° inclination angle, both the shell-side heat transfer coefficient and the overall comprehensive index were well improved [62].

Yang et al. made a new attempt on the structure of helical baffles. They designed a new type of countercurrent U-tube heat exchanger – a single-sided trapezoidal helical baffle heat exchanger –, which is superior to traditional heat exchangers in terms of heat transfer coefficient, resistance, anti-vibration, and anti-fouling [63]. Gu et al. manually reduced the wear of the sharp angle of the inclined baffle hole made by the two-dimensional laser beam cutting machine to the pipeline, and adopted the axial separation of the small inclined angle spiral baffle, which had obvious advantages for the heat transfer coefficient, overall comprehensive index, and temperature uniformity compared to the

traditional segmented baffle [64]. Building on these advancements, Guo et al. simulated continuous spiral schemes with different pitches (50, 110, 160, and 210 mm), and found that an electric heater with a 110 mm pitch had the best overall comprehensive performance, with efficiency improvements ranging from 2.79 to 3.75 times compared to an electric heater with a 210 mm pitch [65]. Through continuous improvement and simulation of the structure of the heat exchanger, Wang et al. developed a continuous helical baffle double-shell downhole electric heater. Experimental results indicated that while the influence of pitch, mass flow, and heating power on the electric heater gradually decreased, the pitch remained a significant factor affecting the heating efficiency of this advanced downhole electric heater [66].

Shinde et al. improved the heat transfer coefficient of the new baffle material FRP (fiber reinforced plastic) by 8–10%, and discovered that larger helix angles (30, 38, and 50°) led to lower heat transfer and reduced pressure drop, while smaller helix angles (10, 19, and 21°) resulted in higher heat transfer and increased pressure drop [67]. Cao et al. proposed an improved scheme of hexagonal helical baffles to reduce the triangular leakage loss at the connecting groove of the adjacent baffles of the commonly used quadrilateral helical baffles, which provided a theoretical basis for the design and optimization of the new heat exchanger [68]. Chen et al. verified this by simulating the performance characteristics of hexagonal spiral heat exchangers with two different angles, and comparing them with trisection heat exchangers with the same pitch or the same tilt angle. Their findings showed that the performance of the heat exchanger is related to its pitch and has nothing to do with the tilt angle of the baffle [69]. Furthermore, Chen et al. used a new type of single-sided trapezoidal helical baffle shell-and-tube heat exchanger to replace the traditional segmental baffle shell-and-tube heat exchanger. Their results demonstrated that the heat transfer coefficient of the unit pressure drop shell side was 151.9–176.4% higher than that of the segmental baffle [70].

In conclusion, optimizing the composition and configuration of electric heaters can effectively enhance the efficiency of electric heating technology. While current advancements in technology primarily rely on simulations and lack practical validation, ongoing research endeavors will enable researchers to further optimize the economic viability of in situ oil shale electric heating technology, leading to its widespread adoption in oil shale mining. In the future, in situ oil shale mining technology will integrate multiple in situ mining techniques to achieve heightened thermal efficiency.

#### 4. Conclusions

This article commences with an exploration of the background of oil shale resource development, and presents the significance and benefits of using electric heating in situ conversion technology. It subsequently outlines the

thermal decomposition mechanism, pore and mineral evolution, scientific research methodologies pertaining to electric heating in situ conversion technology, as well as the categorization of this technology. Lastly, it delves into research on enhancing oil shale electric heating technology.

1. Oil shale can create numerous pores and fractures ranging from microscopic to macroscopic scales through thermal cracking and kerogen pyrolysis. These pores and fractures facilitate the extraction of oil and gas, as well as the establishment of fluid pathways from heating wells to production wells, thereby enhancing shale oil pyrolysis.
2. Although current electric heater heating efficiency optimization relies heavily on digital simulation, the potential enhancement of this efficiency lies in optimizing well geometry and refining electric heater material and structure. As research progresses, these advancements will be integrated to develop more efficient and cost-effective in situ oil shale mining technologies. These technologies may not solely rely on electric heating but could also involve a combination of multiple in situ mining techniques.

## Acknowledgments

This research was financed by the Educational Department of the Liaoning Province for the study of energy coupling mechanism of pulsed plasma fracturing oil shale (No. LJKMZ20220732). We thank the editors and reviewers for their useful feedback that improved this paper. The publication costs of this article were partially covered by the Estonian Academy of Sciences.

## References

1. Li, Y., Chiu, Y.-H., Lin, T.-Y. Research on new and traditional energy sources in OECD countries. *Int. J. Environ. Res. Public Health*, 2019, **16**(7), 1122.
2. Wang, L., Liu, K., Han, B., Shi, H. Accelerated adjustment to a changing international oil market. *Int. Petrol. Econ.*, 2024, **32**(5), 71–77.
3. Jia, C. Z., Zheng, M., Zhang, Y. F. Unconventional hydrocarbon resources in China and the prospect of exploration and development. *Pet. Explor. Dev.*, 2012, **39**(2), 139–146.
4. Taheri-Shakib, J., Kantzas, A. A comprehensive review of microwave application on the oil shale: prospects for shale oil production. *Fuel*, 2021, **305**, 121519.
5. Zhang, Z. J., Chai, J., Zhang, H. Y., Guo, L., Zhan, J.-H. Structural model of Longkou oil shale kerogen and the evolution process under steam pyrolysis based on ReaxFF molecular dynamics simulation. *Energy Sources A: Recovery, Util. Environ. Eff.*, 2021, **43**(2), 252–265.
6. Crawford, P. M., Killen, J. C. New challenges and directions in oil shale development technologies. In: *Oil shale: A Solution to the Liquid Fuel Dilemma* (Hartstein, A. M., Oguniola, O., eds). ACS Publications, Washington, 2010, 21–60.

7. Zafar, A., Su, Y., Wang, W., Alam, S. G., Khan, D., Yasir, M., Alrassas, A., Ahmad, I. Heat dissipation modeling of in-situ conversion process of oil shale. *Open J. Yangtze Oil Gas*, 2020, **5**(2), 46–53.
8. Song, X., Zhang, C., Shi, Y., Li, G. Production performance of oil shale in-situ conversion with multilateral wells. *Energy*, 2019, **189**, 116145.
9. Wang, Y., Wang, Y., Meng, X., Su, J., Li, F., Li, Z. Enlightenment of American's oil shale in-situ retorting technology. *Oil Drill. Prod. Technol.*, 2014, **35**(6), 55–59.
10. World Energy Council. *Survey of Energy Resources*. London, UK, 2010.
11. Zhen, S. *Study on the Characteristics of Temperature Distribution and its Influence on the In Situ Heating Process for Oil Shale*. PhD thesis. Northeast Petroleum University, China, 2024.
12. Lü, X. S., Sun, Y. H., Lu, T., Bai, F., Viljanen, M. An efficient and general analytical approach to modelling pyrolysis kinetics of oil shale. *Fuel*, 2014, **135**, 182–187.
13. He, L., Ma, Y., Yue, C. T., Wu, J., Li, S. Kinetic modeling of Kukersite oil shale pyrolysis with thermal bitumen as an intermediate. *Fuel*, 2020, **279**, 118371.
14. Lei, J., Pan, B. Z., Guo, Y. H., Fan, Y. F., Xue, L. F., Deng, S. H., Zhang, L. H., Ruhan, A. A comprehensive analysis of the pyrolysis effects on oil shale pore structures at multiscale using different measurement methods. *Energy*, 2021, **227**, 120359.
15. Li, Q. *Simulation of Temperature Field and Experiment of In Situ Oil Shale Pyrolysis*. PhD thesis. Jilin University, China, 2012.
16. Han, X. X., Kulaots, I., Jiang, X. M., Suuberg, E. M. Review of oil shale semicoke and its combustion utilization. *Fuel*, 2014, **126**, 143–161.
17. Saif, T., Lin, Q. Y., Butcher, A. R., Bijeljic, B., Blunt, M. J. Multi-scale multi-dimensional microstructure imaging of oil shale pyrolysis using X-ray microtomography, automated ultra-high resolution SEM, MAPS Mineralogy and FIB-SEM. *Appl. Energy*, 2017, **202**, 628–647.
18. Saif, T., Lin, Q. Y., Singh, K., Bijeljic, B., Blunt, M. J. Dynamic imaging of oil shale pyrolysis using synchrotron X-ray microtomography. *Geophys. Res. Lett.*, 2016, **43**(13), 6799–6807.
19. Saif, T., Lin, Q. Y., Bijeljic, B., Blunt, M. J. Microstructural imaging and characterization of oil shale before and after pyrolysis. *Fuel*, 2017, **197**, 562–574.
20. Tiwari, P., Deo, M., Lin, C., Miller, J. D. Characterization of oil shale pore structure before and after pyrolysis by using X-ray micro CT. *Fuel*, 2013, **107**, 547–554.
21. He, W. T., Sun, Y. H., Shan, X. L. Organic matter evolution in pyrolysis experiments of oil shale under high pressure: guidance for in situ conversion of oil shale in the Songliao Basin. *J. Anal. Appl. Pyrolysis*, 2021, **155**, 105091.
22. Bai, F. T., Sun, Y. H., Liu, Y. M., Guo, M. G. Evaluation of the porous structure of Huadian oil shale during pyrolysis using multiple approaches. *Fuel*, 2017, **187**, 1–8.

23. Kang, Z. Q., Yang, D., Zhao, Y. S., Hu, Y. Q. Thermal cracking and corresponding permeability of Fushun oil shale. *Oil Shale*, 2011, **28**(2), 273–283.
24. You, Y., Wang, X., Han, X., Jiang, X. Kerogen pyrolysis model based on its chemical structure for predicting product evolution. *Fuel*, 2019, **246**, 149–159.
25. Crawford, P. M., Biglarbigi, K., Dammer, A. R., Knaus, E. Advances in world oil shale production technologies. In: *SPE Annual Technical Conference and Exhibition*, September 21–24, 2008, Denver, USA. OnePetro, 2008.
26. Prats, M., Meurs, P. van. *Method of Producing Fluidized Material from a Subterranean Formation*. Patent US8104536B2, 1969-07-15.
27. Prats, M., Closmann, P. J., Ireson, A. T., Drinkard, G. Soluble-salt processes for in-situ recovery of hydrocarbons from oil shale. *J. Pet. Technol.*, 1977, **29**(9), 1078–1088.
28. Kang, Z., Zhao, Y., Yang, D. Review of oil shale in situ conversion technology. *Appl. Energy*, 2020, **269**, 115121.
29. Tanaka, P., Yeakel, J., Symington, W., Spiecker, P. M., Del Pico, M., Thomas, M. M., Sullivan, K. B., Stone, M. T. Plan to test ExxonMobil's in situ oil shale technology on a proposed RD&D lease. In: *31st Oil Shale Symposium*, October 17–19, 2011, Colorado School of Mines, Golden, Colorado.
30. Michaels, J. A., Wood, D. R., Froeter, P. J., Huang, W., Sievers, D. J., Li, X. Effect of perforation on the thermal and electrical breakdown of self-rolled-up nanomembrane structures. *Adv. Mater. Interfaces*, 2019, **6**(21), 1901022.
31. Li, J. S., Sun, Y. H., Guo, W., Li, Q., Deng, S. H. Laboratory test of oil shale pyrolysis by high voltage-power frequency electric heating and the analysis on oxygen driving effect. *Drill. Eng.*, 2018, **45**(5), 13–17.
32. Wang, J. *Numerical Simulation of Temperature Field for the In-situ Upgrading of Oil Shale*. Master's thesis. Jilin University, China, 2011.
33. Fan, Y. Q., Durlofsky, L. J., Tchelepi, H. A. Numerical simulation of the in-situ upgrading of oil shale. *SPE J.*, 2010, **15**(2), 368–381.
34. Xia, T. *Research on In-situ Electrical Heating Development of Oil Shale Reservoir by Numerical Simulation*. PhD thesis. China University of Petroleum, China, 2015.
35. Li, X. X. *Numerical Simulation of Temperature Field In Situ Modified by Electric Heating of Oil Shale*. PhD thesis. Northeast Petroleum University, China, 2021.
36. Pei, S. F., Wang, Y. Y., Zhang, L., Huang, L. J., Cui, G. D., Zhang, P. F., Ren, S. R. An innovative nitrogen injection assisted in-situ conversion process for oil shale recovery: mechanism and reservoir simulation study. *J. Pet. Sci. Eng.*, 2018, **171**, 507–515.
37. Meng, X. L., Bian, J. J., Li, J., Ma, Z. L., Long, Q. L., Su, J. Z. Porous aluminosilicates catalysts for low and medium matured shale oil in situ upgrading. *Energy Sci. Eng.*, 2020, **8**(8), 2859–2867.
38. Sun, C. L., Wang, Y., Shao, H. L., An, J. N., Zhao, Y. D., Yang, Q. R. Numerical simulation of the development of oil shale in situ electrical temperature field. *J. Liaoning Univ. Pet. Chem. Technol.*, 2015, **35**(4), 40–43.
39. Yue, C. T., Liu, Y., Ma, Y., Li, S. Y., He, J. L., Qiu, D. K. Influence of retorting

- conditions on the pyrolysis of Yaojie oil shale. *Oil Shale*, 2014, **31**(1), 66–78.
40. Wang, Q., Sun, B., Hu, A., Bai, J., Li, S. Pyrolysis characteristics of Huadian oil shales. *Oil Shale*, 2007, **24**(2), 147–157.
  41. Vinegar, H. J., Bass, R. M., Hunsucker, B. *Heat Sources with Conductive Material for In Situ Thermal Processing of an Oil Shale Formation*. Patent US20040211554A1, 2005-08-16.
  42. Hoekstra, E., Swaaij, W. P. van, Kersten, S. R. A., Hogendoorn, K. J. A. Fast pyrolysis in a novel wire-mesh reactor: design and initial results. *Chem. Eng. J.*, 2012, **191**, 45–58.
  43. Zeng, G. Y., Wang, C. X., Yang, H. Simulation and design optimization of temperature distribution of in-situ heating electric heater for oil shale. *Oil Drill. Prod. Technol.*, 2014, **36**(5), 84–89.
  44. Sandberg, C., Thomas, K., Penny, S. The use of coiled tubing for deployment of electrical heaters in downhole applications. In: *SPE/ICoTA Coiled Tubing and Well Intervention Conference and Exhibition*, March 22–23, 2016, Houston, USA. OnePetro, 2016.
  45. Hao, Y. A composite cementing material with high-temperature and high-pressure resistance and low elasticity for in-situ heating of oil shale. *Chem. Technol. Fuels Oils*, 2016, **52**, 103–110.
  46. Gao, X. Q., Yang, H., Xiong, F. S., Lv, J. G. Temperature field and thermal stress of downhole system for in situ heating on oil shale. *Fault-Block Oil Gas Field*, 2014, **21**(3), 373–377.
  47. Lei, Y.-G., He, Y.-L., Chu, P., Li, R. Design and optimization of heat exchangers with helical baffles. *Chem. Eng. Sci.*, 2008, **63**(17), 4386–4395.
  48. Wang, Q.-W., Chen, G.-D., Xu, J., Ji, Y.-P. Second-law thermodynamic comparison and maximal velocity ratio design of shell-and-tube heat exchangers with continuous helical baffles. *J. Heat Transf.*, 2010, **132**(10), 101801.
  49. Zhang, J.-F., Li, B., Huang, W.-J., Lei, Y.-G., He, Y.-L., Tao, W.-Q. Experimental performance comparison of shell-side heat transfer for shell-and-tube heat exchangers with middle-overlapped helical baffles and segmental baffles. *Chem. Eng. Sci.*, 2009, **64**(8), 1643–1653.
  50. Xiao, X., Zhang, L., Li, X., Jian, B., Yang, X., Xia, Y. Numerical investigation of helical baffles heat exchanger with different Prandtl number fluids. *Int. J. Heat Mass Transf.*, 2013, **63**, 434–444.
  51. Yang, J.-F., Zeng, M., Wang, Q.-W. Effects of sealing strips on shell-side flow and heat transfer performance of a heat exchanger with helical baffles. *Appl. Therm. Eng.*, 2014, **64**(1–2), 117–128.
  52. Wang, S., Wen, J., Yang, H., Xue, Y., Tuo, H. Experimental investigation on heat transfer enhancement of a heat exchanger with helical baffles through blockage of triangle leakage zones. *Appl. Therm. Eng.*, 2014, **67**(1–2), 122–130.
  53. Dong, C., Chen, Y.-P., Wu, J.-F. Flow and heat transfer performances of helical baffle heat exchangers with different baffle configurations. *Appl. Therm. Eng.*, 2015, **80**, 328–338.
  54. Chen, Y.-P., Sheng, Y.-J., Dong, C., Wu, J.-F. Numerical simulation on flow

- field in circumferential overlap trisection helical baffle heat exchanger. *Appl. Therm. Eng.*, 2013, **50**(1), 1035–1043.
55. Dong, C., Chen, Y., Wu, J. Performances of helical baffle heat exchangers with different baffle assembly configurations. *Can. J. Chem. Eng.*, 2015, **93**(8), 1500–1508.
  56. Dong, C., Chen, Y.-P., Wu, J.-F. Influence of baffle configurations on flow and heat transfer characteristics of trisection helical baffle heat exchangers. *Energy Convers. Manag.*, 2014, **88**, 251–258.
  57. Dong, C., Chen, Y., Wu, J. Comparison of heat transfer performances of helix baffled heat exchangers with different baffle configurations. *Chin. J. Chem. Eng.*, 2015, **23**(1), 255–261.
  58. Yang, J.-F., Zeng, M., Wang, Q.-W. Numerical investigation on combined single shell-pass shell-and-tube heat exchanger with two-layer continuous helical baffles. *Int. J. Heat Mass Transf.*, 2015, **84**, 103–113.
  59. El Maakoul, A., Lahnizi, A., Saadeddine, S., El Metoui, M., Zaitte, A., Meziane, M., Ben Abdellah, A. Numerical comparison of shell-side performance for shell and tube heat exchangers with trefoil-hole, helical and segmental baffles. *Appl. Therm. Eng.*, 2016, **109**(A), 175–185.
  60. Dong, C., Li, D., Zheng, Y., Li, G., Suo, Y., Chen, Y. An efficient and low resistant circumferential overlap trisection helical baffle heat exchanger with folded baffles. *Energy Convers. Manag.*, 2016, **113**, 143–152.
  61. Yang, J.-F., Lin, Y.-S., Ke, H.-B., Zeng, M., Wang, Q.-W. Investigation on combined multiple shell-pass shell-and-tube heat exchanger with continuous helical baffles. *Energy*, 2016, **115**, 1572–1579.
  62. Chen, Y., Cao, R. B., Dong, C., Wu, J. F., Wang, M. C. Numerical simulation on the performance of trisection helical baffle heat exchangers with small baffle incline angles. *Numer. Heat Transf.; A: Appl.*, 2016, **69**(2), 180–194.
  63. Yang, S., Chen, Y., Wu, J., Gu, H. Performance simulation on unilateral ladder type helical baffle heat exchanger in half cylindrical space. *Energy Convers. Manag.*, 2017, **150**, 134–147.
  64. Gu, H., Chen, Y., Wu, J., Yang, S. Numerical study on performances of small incline angle helical baffle electric heaters with axial separation. *Appl. Therm. Eng.*, 2017, **126**, 963–975.
  65. Guo, W., Wang, Z. D., Sun, Z. J., Sun, Y. H., Lü, X. S., Deng, S. H., Qu, L., Yuan, W., Li, Q. Experimental investigation on performance of downhole electric heaters with continuous helical baffles used in oil shale in situ pyrolysis. *Appl. Therm. Eng.*, 2019, **147**, 1024–1035.
  66. Wang, Z. D., Lü, X. S., Li, Q., Sun, Y. H., Wang, Y., Deng, S. H., Guo, W. Downhole electric heater with high heating efficiency for oil shale exploitation based on a double-shell structure. *Energy*, 2020, **211**, 118539.
  67. Shinde, S., Chavan, U. Numerical and experimental analysis on shell side thermo-hydraulic performance of shell and tube heat exchanger with continuous helical FRP baffles. *Therm. Sci. Eng. Prog.*, 2018, **5**, 158–171.
  68. Cao, X., Du, T., Liu, Z., Zhai, H., Duan, Z. Experimental and numerical

- investigation on heat transfer and fluid flow performance of sextant helical baffle heat exchangers. *Int. J. Heat Mass Transf.*, 2019, **142**, 118437.
69. Chen, J., Lu, X., Wang, Q., Zeng, M. Experimental investigation on thermal-hydraulic performance of a novel shell-and-tube heat exchanger with unilateral ladder type helical baffles. *Appl. Therm. Eng.*, 2019, **161**(9), 114099.
  70. Chen, Y., Tang, H., Wu, J., Gu, H., Yang, S. Performance comparison of heat exchangers using sextant/trisection helical baffles and segmental ones. *Chin. J. Chem. Eng.*, 2019, **27**(12), 2892–2899.